

Article

Inline Weld Depth Evaluation and Control Based on OCT Keyhole Depth Measurement and Fuzzy Control

Maximilian Schmoeller *, Tony Weiss, Korbinian Goetz, Christian Stadter , Christian Bernauer 
and Michael F. Zaeh

Institute for Machine Tools and Industrial Management, TUM School of Engineering and Design, Technical University of Munich, 85748 Garching, Germany; tony.weiss@iwb.tum.de (T.W.); korbinian.goetz@tum.de (K.G.); christian.stadter@iwb.tum.de (C.S.); christian.bernauer@iwb.tum.de (C.B.); michael.zaeh@iwb.tum.de (M.F.Z.)

* Correspondence: maximilian.schmoeller@iwb.tum.de; Tel.: +49-89-289-55474

Abstract: In an industrial joining process, exemplified by deep penetration laser beam welding, ensuring a high quality of welds requires a great effort. The quality cannot be fully established by testing, but can only be produced. The fundamental requirements for a high weld seam quality in laser beam welding are therefore already laid in the process, which makes the use of control systems essential in fully automated production. With the aid of process monitoring systems that can supply data inline to a production process, the foundation is laid for the efficient and cycle-time-neutral control of welding processes. In particular, if novel, direct measurement methods, such as Optical Coherence Tomography, are used for the acquisition of direct geometric quantities, e.g., the weld penetration depth, a significant control potential can be exploited. In this work, an inline weld depth control system based on an OCT keyhole depth measurement is presented. The system is capable of automatically executing an inline control of the deep penetration welding process based only on a specified target weld depth. The performance of the control system was demonstrated on various aluminum alloys and for different penetration depths. In addition, the ability of the control to respond to unforeseen external disturbances was tested. Within the scope of this work, it was thus possible to provide an outlook on future developments in the field of laser welding technology, which could develop in the direction of an intuitive manufacturing process. This objective should be accomplished through the use of intelligent algorithms and innovative measurement technology—following the example of laser beam cutting, where the processing systems themselves have been provided with the ability to select suitable process parameters for several years now.



Citation: Schmoeller, M.; Weiss, T.; Goetz, K.; Stadter, C.; Bernauer, C.; Zaeh, M.F. Inline Weld Depth Evaluation and Control Based on OCT Keyhole Depth Measurement and Fuzzy Control. *Processes* **2022**, *10*, 1422. <https://doi.org/10.3390/pr10071422>

Academic Editor: Jie Zhang

Received: 23 June 2022

Accepted: 19 July 2022

Published: 21 July 2022

Publisher's Note: MDPI stays neutral with regard to jurisdictional claims in published maps and institutional affiliations.



Copyright: © 2022 by the authors. Licensee MDPI, Basel, Switzerland. This article is an open access article distributed under the terms and conditions of the Creative Commons Attribution (CC BY) license (<https://creativecommons.org/licenses/by/4.0/>).

Keywords: optical coherence tomography; inline weld depth evaluation; inline weld depth control; laser beam welding; machine learning; wavelet transformation; fuzzy control

1. Introduction

Laser beam welding offers the potential for safe, efficient and highly automated production due to the high weld seam quality and productivity that can be achieved. An essential prerequisite for the use of the technology in industrial manufacturing is the ability to ensure and comprehensively document product quality. Since joining processes are typically performed at a late stage of the value chain, for example, in the production of electric energy storage devices, very low defect rates must be achieved. Inline process monitoring systems can be used to detect defective joints caused by irregularities in the welding process. The data obtained offer great potential for reducing rejects by improving and stabilizing the production processes. For this, inline control systems that adaptively adjust the process are an efficient method. These can help to make the transition from the detection to the prevention of an inadequate product quality. Laser beam welding is characterized by a concentrated energy input and thus a small heat-affected zone during the

joining process compared to other fusion welding processes. Above a threshold intensity of laser radiation, the evaporation temperature of metallic materials is exceeded. This leads to the formation of a so-called keyhole, which is maintained by the high pressure of the metal vapor within the capillary. The resulting deep welding process is characterized by a high degree of efficiency since the laser radiation is reflected several times by the keyhole walls and is partially absorbed at each impact. However, the high temperature gradients lead to dynamic fluctuations in the welding process. If these instabilities lead to a keyhole collapse, spatter ejection or a change in the weld penetration depth may occur. For many technical applications, ensuring a constant weld depth is essential. Weld depth control in deep penetration laser beam welding (DPLW) has been the subject of research for many years. In this context, the development of a precise and real-time, capable method for inline measurement of the penetration depth is of great importance. One possible solution is based on an interferometric sensing principle, meaning Optical Coherence Tomography (OCT), in which a measuring laser beam is directed to the process zone coaxially to the processing laser beam [1]. This sensor technology enables a keyhole depth measurement with a frequency of several kilohertz and an axial accuracy in the range of a few micrometers. However, the sensor signal is strongly influenced by the dynamic variations of the keyhole, by the material of the parts to be joined and by the process parameters. This results in an inherent challenge regarding the interpretation of the OCT measurement signal.

2. State of the Art

In the following sections, the state of the art in research and technology for process monitoring in laser beam welding applications is presented with a detailed consideration of the weld depth measurement using Optical Coherence Tomography (OCT). In addition, approaches to data processing and interpretation in process monitoring systems are reviewed with a focus on Artificial-Intelligence-based systems. Finally, existing approaches for the control of deep penetration laser beam welding processes by selectively influencing the process parameters are discussed.

2.1. *Inline Weld Depth Measurement for Deep Penetration Laser Beam Welding*

In the research field of laser process monitoring, a wide range of optical sensor approaches [2–4] were investigated to enable inline monitoring and a closed-loop control of the process [5]. Within the referenced scientific studies, correlations between the evaluated sensor signals and the welding depth were examined. Given the growing need for inline process monitoring regarding quality assurance in welding technology, OCT sensor concepts represent a suitable technology. By using OCT, highly accurate surface topography measurements with a temporal resolution of up to several kilohertz are obtainable independent of the process emissions during welding, which was first presented by Bautze and Kogel-Hollacher [6]. For the inline evaluation of the weld depth during deep penetration welding, the OCT sensor signal allows for direct conclusions about the stability of the welding process [7]. Schmoeller et al. [8], Kogel-Hollacher et al. [9], Sokolov et al. [10] and Webster et al. [11] demonstrated the applicability of an OCT-based sensor for the measurement of the keyhole depth, the keyhole position mapping in micro laser beam welding and the 3D surface measurement in remote laser ablation, respectively. Fundamental insights regarding the relationship between the keyhole geometry in laser beam welding and the signal from OCT-based keyhole depth measurements were presented by Stadter et al. [12]. For this, they used a ray-tracing approach to numerically reproduce the propagation paths of the measurement radiation within the vapor capillary.

2.2. *Artificial Intelligence in Laser Welding Applications*

With increasing computational performance, the integration of Artificial Intelligence (AI) solutions into laser material processing applications is becoming attainable in the context of the real-time capability of technical systems. Possible applications are in the area of monitoring the welding process, e.g., the prediction of the weld seam quality [7]

or the optimization of the welding parameters [13]. Günther et al. [14] presented a system architecture which addresses different domains of a laser welding system. A high-speed camera system and photodiodes were used for process monitoring. Machine Learning (ML) algorithms such as a Deep Neural Network-based autoencoder for feature extraction as well as a self-learning system controller were implemented for data evaluation. Other research [2,15] focused on camera-based quality monitoring and evaluation of the welding process in various applications such as weld seam classification and defect detection. In these cases, Neural Networks, especially Convolutional Neural Networks, were identified as a suitable technique for image processing [2] or general welding process state determination [15]. The full potential of AI for data analysis in welding applications could be achieved by combining different techniques, as demonstrated by Zhang et al. [16], who used a Deep Neural Network for processing the welding data and modeled the relationship between sensor data features and the welding process behavior. Furthermore, a genetic algorithm and a backpropagation Neural Network were applied to optimize and evaluate the parameters of the first network, i.e., the network for data processing.

2.3. Process Control in Deep Penetration Laser Beam Welding

Blug et al. [17] developed a control strategy based on an optical signal detecting the full penetration hole (FPH). The FPH is formed during the capillary breakthrough of the upper joining partner in overlap welds. The signal was evaluated by a Cellular Neural Network (CNN), resulting in a defined detection rate, i.e., the occurrence rate of the FPH, i.e., the temporal frequency of the occurrence of a full penetration. A two-stage control loop was defined using the detection rate as the controlled variable. As proposed in Blug et al. [18], the fast component controlled the laser power in fixed steps of ± 50 W, achieving the required FPH detection rate. The second component defined the power range in which the laser power was varied. To ensure a constant full penetration of two sheets in an overlap configuration, Bardin et al. [19] presented a proportional (P) controller based on the evaluation of camera images. The brightness of the keyhole region indicated the penetration of the joining partners. Deviations from an experimentally quantified operating point were compensated by a linear adjustment of the laser power. Furthermore, the authors determined that the laser power does not follow the complete process window linearly, so the control is limited to a fixed range of sheet thicknesses. Birnesser [20] proposed a proportional-integral-derivative (PID) controller based on an optical sensor signal. The author correlated the intensity of the infrared radiation emitted from the process zone, measured by a spectrometer, with the weld depth. The control error between the filtered value of the infrared signal and an external setpoint was used to manipulate the laser power. Konuk et al. [21] correlated the keyhole depth with the temperature above the process zone, determined with an optical sensor for temperature measurement. The authors chose a proportional-integral (PI) controller. Based on the control error, determined by the deviation between an experimentally identified operating point and a constant electron temperature, the laser power was adjusted by the controller. However, it was identified that the electron temperature is sensitive to the experimental setup and must be thoroughly calibrated before executing the experiment. Kos et al. [22] correlated camera images of the interaction zone with the weld depth. Linear behavior of the weld depth was shown for a partially penetrating process during remote laser beam welding. The calculated laser power from the corresponding size of the interaction zone, extracted from the camera images, represented the input for a feed-forward PI control loop. Based on a keyhole approximation model of Michel [23], Bollig et al. [24] presented a model predictive control with a controller frequency of 500 Hz. The control algorithm aimed to preset the targeted laser power as a function of the predicted feed rate, resulting in a quality function. As the mathematical minimization problem was convex, the linearly approximated controller was validated around an operating point based on the feed rate variation. To transfer human expert knowledge in manufacturing to the control of tungsten inert gas welding (TIG), Liu et al. [25] provided an approach for a process model based on fuzzy logic. The TIG process

was controlled using the current as the manipulated variable to keep the penetration depth constant. Using an optical image sensor to monitor the weld pool and the subsequent reaction of the welder, i.e., the parameter adjustment, a process model was determined. The process model was implemented in a closed-loop control by transferring the parameters into a fuzzy logic.

3. Objectives and Approach

In this paper, an inline weld depth control system is presented. It is based on adaptive data processing methods for the interpretation of the keyhole measurement signal with respect to the weld depth. In order to use the signals from an OCT sensor as input signals for the weld depth control, a deep understanding of the measurement process and the process-determining variables in deep penetration laser beam welding (DPLW) is required. The influences on the OCT signal and the thickness of the melt layer, i.e., the physical difference between the keyhole and the weld depth, are the basis for data interpretation. Machine Learning methods are used to provide regression of the structured data. To control the DPLW process, in addition to a well-understood input signal, an accurate knowledge of the possible responses, i.e., control reactions, to actively influence the weld depth is required. In particular, ML methods are used to evaluate the relationships between the process parameters and the weld depth. Extensive training datasets must be obtained to apply ML methods to process inline measurement data. Computed tomography (CT) images of weld specimens provide a comprehensive dataset that can be compared with inline evaluated weld depths as reference data. Based on the knowledge obtained, a closed-loop weld depth control for DPLW was implemented.

4. Materials and Methods

4.1. Experimental Setup

A laser beam welding system was used within this work, which was developed for the specific purpose of inline weld depth control. The system was characterized by a full time synchronization between signals of a process monitoring system and the control signals for the significant process-influencing components. The core of the setup was the programmable logic controller (PLC), which processed all measurement and control signals and provided them with a time stamp. The process control system was implemented within the PLC, which allowed for an adjustment of the process parameters depending on the measured controlled variables. Fixed laser welding optics of the type YW52 (Precitec GmbH & Co. KG, Gaggenau, Germany) with an image ratio of 1:1 were used. The component movement and the welding optics' positioning were carried out by a 3-axis CNC system at a maximum speed of 12 m/min. It served to adjust the distance between the focal point and the component as well as to move the component relative to the fixed operating point of the optics. Three synchronous servo motors were used for the axis movements, which returned their respective positions to the controller in real time. The data obtained were used, for example, to determine the actual feed rate of the component in the x–y plane, which may deviate slightly from the specified value due to external influences. A continuous-wave (cw) multi-mode fiber laser (FL080, Coherent Inc., Santa Clara, CA, USA) with a maximum power of 8 kW and a fiber core diameter of 100 µm provided the laser radiation for the processing, guided into the optics in an optical fiber. The laser beam source was integrated into the control loop as well, in which it received a power setpoint from the control system and returned the actual value. In addition, an OCT-based inline process monitoring system (IDM 1.1, Precitec GmbH & Co. KG, Gaggenau, Germany) was integrated into the welding system. It measured the distance between the processing optics and a specific point on the component. The OCT sensor transmitted distance values in the form of two analog signals, containing information on the position of the capillary ground and the component surface in order to determine the capillary depth from the difference, to the PLC, which recorded and synchronized them with all other recorded process variables. Figure 1 shows the schematic structure of the laser beam

welding system and the information streams transmitted in the form of light, digital signals or analog signals.

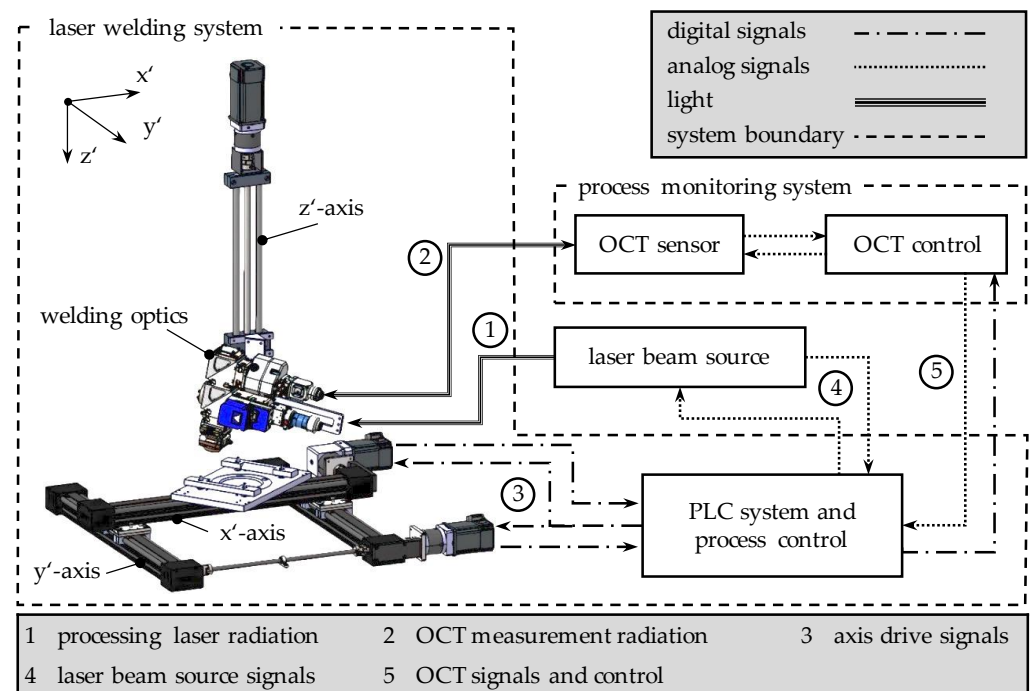


Figure 1. System architecture of the laser welding system with weld depth control and data streams within the system.

4.2. Materials and Specimens

The sample geometry in Figure 2 (left side) was used for the main experiments to obtain reference data and to develop the controller structure. To design the ML approach for determining the weld depth based on the OCT keyhole depth measurement data (Section 5.1), the generated training data were employed. The notch depicted, with a depth and length of 1 mm, was used to generate a reference for matching the process signals with the depth obtained from the microfocus computed tomography (μ CT) scans [26], in addition to the trigger signal based on the laser emission switch-on time. As a sample material, the aluminum base alloy AA2219 was chosen. The second sample geometry (Figure 2, right side) was used for the validation experiments. A notch with a total length of 50 mm and a depth of 300 μ m was milled in the center of the EN AW-6082 and AA2219 specimens, creating an external disturbance that was not detected by the OCT reference beam, as the reference beam was directed to the surface of the welding fixture. EN AW-6082 was chosen as a validation material with different material properties compared to AA2219. Thus, the disturbance variable only affected the keyhole depth measurement signal. The notch, therefore, represented a sudden increase in the weld depth of the evaluation algorithm. Such deviations might, for example, occur as a result of a heat accumulation. Accordingly, the weld depth control had to compensate for the external disturbance and reduce the laser power to realign the target and the real weld depth. Both sample types had a material thickness of 4 mm.

4.3. Data Processing Methods

By using a discrete wavelet transformation, signals in technical applications, e.g., for pattern recognition or noise reduction, can be processed in a computationally efficient manner [27]. Consisting of two calculation steps, a wavelet transformation decomposes the original signal into approximations a_i and details d_i within the wavelet analysis, and reconstructs the original signal based on those coefficients during the wavelet synthesis [28].

The wavelet analysis is derived from the short-time Fourier analysis [29] and determines the coefficients by breaking up the original signal into shifted and scaled components of the basis function (mother wavelet). The basis function ψ has to fulfill the following two conditions [28]:

$$\int_{-\infty}^{\infty} \psi(t) dt = 0 \quad \int_{-\infty}^{\infty} |\psi(t)|^2 dt < \infty \quad (1)$$

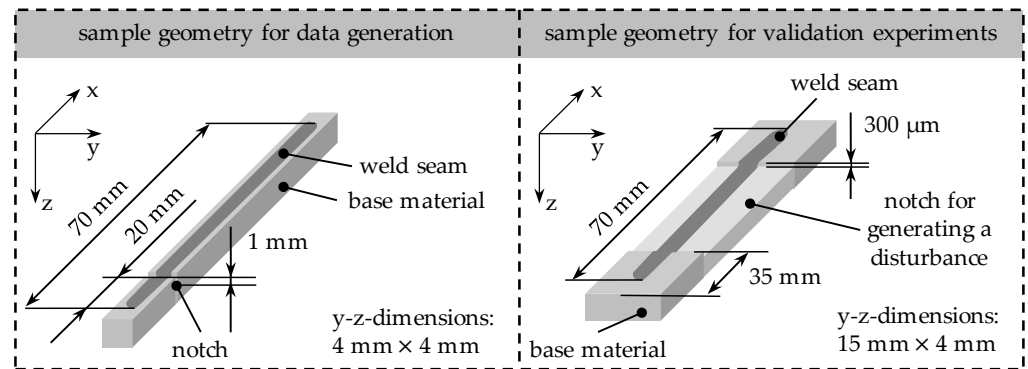


Figure 2. Specimen geometries for the welding experiments; **(left):** specimen geometry for data generation by μ CT with reference notch for the correlation of OCT data and the position of the record along the feed direction; **(right):** specimen geometry for the validation of the weld depth control with a notch on the surface for the generation of a disturbance in the controlled system.

The Haar-wavelet, as an example, is a simple and computationally efficient method to solve orthonormal basis functions that is widely used. It can be expressed with the following characteristics:

$$\psi(t) = \begin{cases} 1 & 0 \leq t < \frac{1}{2} \\ -1 & \frac{1}{2} \leq t < 1 \\ 0 & \text{otherwise} \end{cases} \quad (2)$$

In the presented paper, the Haar-wavelet is used in the context of a discrete wavelet transformation to denoise the OCT depth signal.

5. Structure of the Data Evaluation and Control System

5.1. Inline Weld Depth Evaluation

The OCT sensor used in the experimental setup provided two analog output signals representing the measured distance to the workpiece surface and to the keyhole ground. Both signals were analyzed in a data filtering and cleansing step using a percentile filtering and a wavelet transformation algorithm. In addition, the resulting sampled signal was further processed to extract relevant features in preparation for the weld depth prediction using a Feed Forward Neural Network (FFNN).

The two analog signals from the OCT sensor were transmitted to the connected PLC within a voltage range from 0 V to 10 V. On an EtherCAT-based digital input terminal, the signals were oversampled and digitized at 100 kHz, i.e., 100 data points per signal sampling timeframe of 1 ms were delivered to the PLC. The PLC stored the measured values for each signal over a period of 6 ms in a data array, resulting in two data packages with 600 data points each. The compressed data packages were processed as shown in Figure 3.

To handle the high data rates required for a real-time closed-loop weld depth control, a number of data processing steps were required with the goal of processing the incoming signals with a minimum loss of information and with a short delay. The data processing pipeline in the algorithm was therefore divided into three major sections. Since both the signal component from the keyhole and the surface reference signal are displaced by an equal offset value, the purpose of the first section was to compute a normalized depth signal (Figure 4a). In the first data processing step, a 3% percentile filtering with a sliding

window of a width of 250 data points was applied to convert the raw scattered reference signal, i.e., the surface signal, into a continuous signal. The obtained filtered reference signal was used to normalize the raw depth signal. The depth signal was normalized before it was filtered and converted into a continuous signal to avoid a loss of information in the signal features. For continuity, the reference signal was subtracted from the raw surface reference signal on a data point basis, resulting in a normalized depth signal that was still in the form of scattered measurement points, with no change in signal characteristics. A discrete one-dimensional wavelet transformation was applied to decompose the raw depth signal into approximations a_i and details d_i using a Haar-wavelet as the basis function (Figure 4b). After reconstructing the signal using the obtained coefficients, existing outliers needed to be removed from the signal to obtain a filtered and continuous capillary depth signal (Figure 4c). The remaining outliers were mainly the results of measurement errors and were not related to phenomena of the welding process. Relevant statistical features in the given window, e.g., the standard deviation, were extracted from the signal.

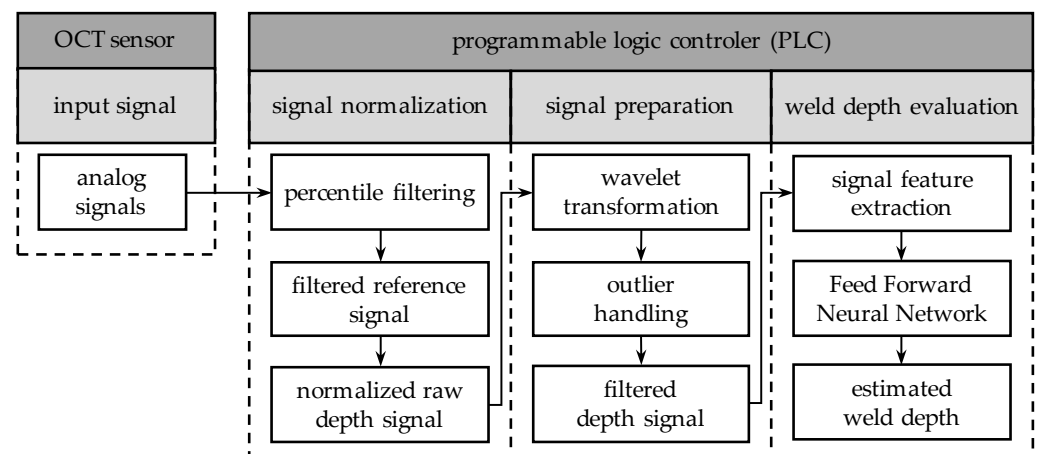


Figure 3. Sequence and data processing steps for the weld depth interpretation based on the analog OCT signals.

Together with the process parameters of the laser power, feed rate and angle of incidence of the welding optics as additional features, a total of nine features represented the input of the FFNN. The laser power and the feed rate showed a significantly strong influence on the welding process. Therefore, these features were weighted accordingly high as inputs for the FFNN. The angle of incidence of the welding optics was kept identical for the main and the validation experiments, but was still included as a feature. In the case of a different welding optics setup in further research experiments, the same FFNN can be used for interpreting the features. In previous studies, Schmoeller et al. [30] evaluated the thickness of the process-parameter-dependent melt layer below the keyhole, which results in the difference between the measured keyhole depth and the depth obtained from metallographic cross-sections. The thickness of the melt layer obtained from a numerical weld pool simulation served as an additional offset for the estimated weld depth from the FFNN. The structure of the fully connected FFNN (cf. Figure 4d) further consisted of two hidden layers with 19 and 17 neurons, respectively, and a one-dimensional output layer. In both hidden layers, the ReLU-function (Rectified Linear Unit) was implemented as an activation function. Based on the features, the FFNN predicted the current weld depth, which was used as an input variable for the control system (Figure 4e).

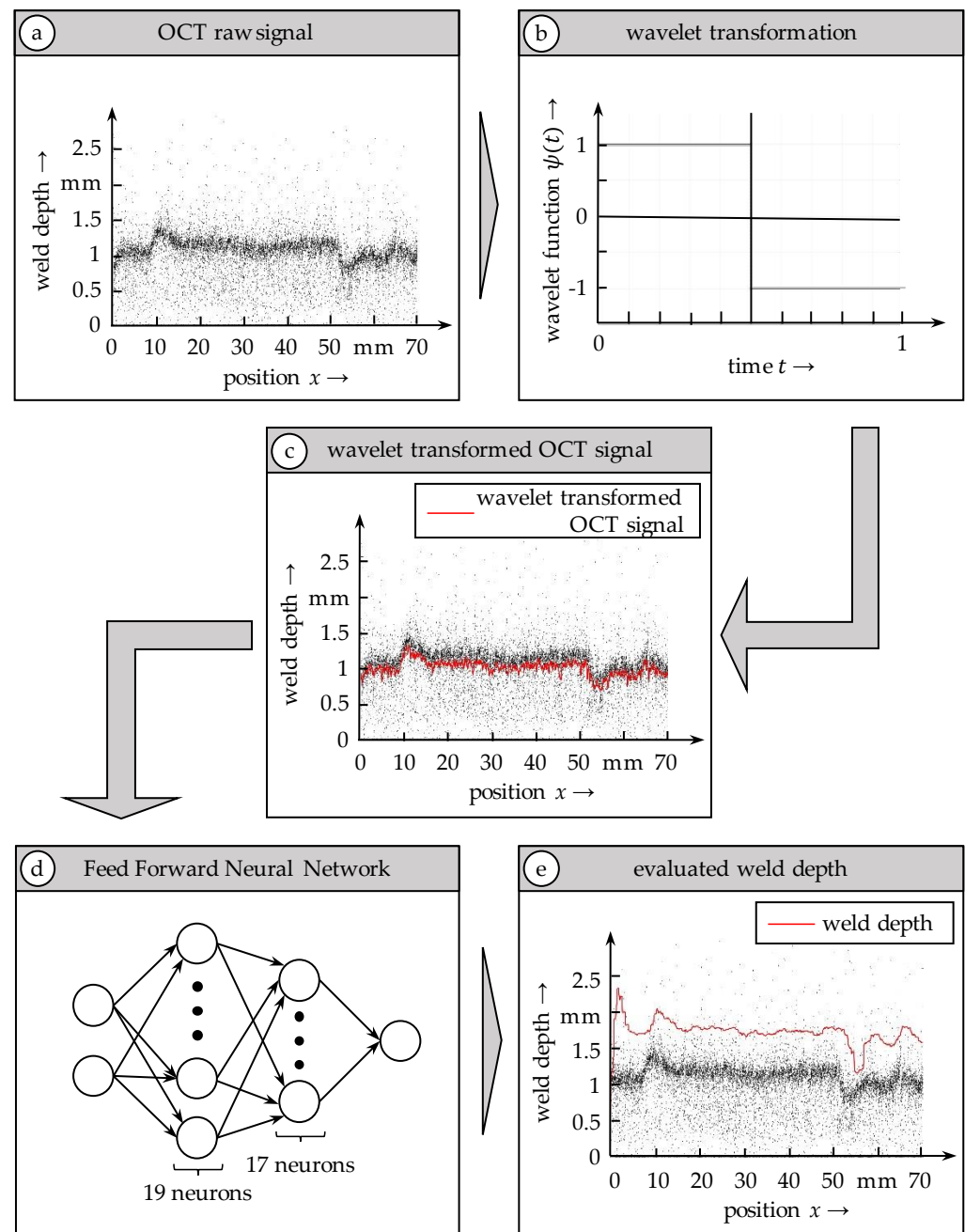


Figure 4. Sequence of the interpretation of the OCT keyhole depth measurement signal with respect to the weld depth, taking into account the identified signal influencing parameters using a wavelet transformation and an FFNN.

5.2. Inline Weld Depth Control

The laser power and the feed rate were both suitable as manipulated variables to control the user-desired weld depth. The adjustment of the laser power allowed for a fast adaptation of the process, as it directly influenced the dynamics of the keyhole, in contrast to the slowly responding mechanics of the feed system [14,17,20]. To characterize the laser power for its usage as a manipulated variable, various step response tests of the laser beam source were carried out (cf. Figure 5). The characteristic of the resulting laser power was measured through the analog interface of the laser beam source. An initial reference laser power of $P_L = 400$ W was chosen. After the target, i.e., the setpoint laser power of $P_{L,s} = 400$ W, was reached, a further step increase of 100 W was applied, serving as an exemplary control action. The system showed a transient behavior with an average

reaction period of $\Delta t = 24$ ms to adjust to the new targeted laser power by the laser beam source after the control signal was sent from the PLC. Additionally, the laser beam source exhibited a constant deviation of $\Delta P = 30$ W below the target laser power. The temporal delay between the setpoint and the actual laser power determined the fastest possible controller response and thus the maximum achievable bandwidth of the control system. Consequently, the sensitivity of the controller was adjusted according to the response time, and the offset of the actual laser power ΔP was compensated.

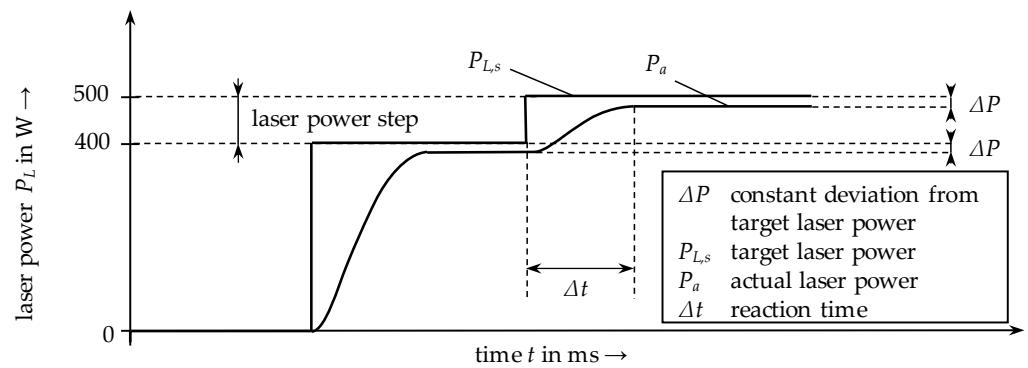


Figure 5. Schematic representation of the response of the actual laser power P_a emitted by the laser beam source to a stepwise change of the specified targeted laser power P_t .

Due to the transient behavior of the feed rate v_w caused by the comparatively slow reaction of the drive axes, the laser power P_L was chosen as the main manipulated variable to control the weld depth. However, Schmoeller et al. [31] and Hagenlocher et al. [32] showed a correlation between higher feed rates and the process stability of deep penetration laser beam welding. The feed rate v_w was therefore used to ensure stable process conditions, resulting in high seam quality.

Based on the data of Schmoeller et al. [31], a linear regression between the weld depth and the feed rate was applied by the pilot control, such that an optimum of high stability for the current operating point was found. A maximum feed rate of 8.5 m/min was chosen, declining for higher targeted weld depths.

Both the pilot control and the fuzzy controller itself contained a process model, which is shown in Figure 6. The modeling of the process behavior during laser beam deep penetration welding of aluminum was based on the experimental process characterization of Schmoeller et al. [31].

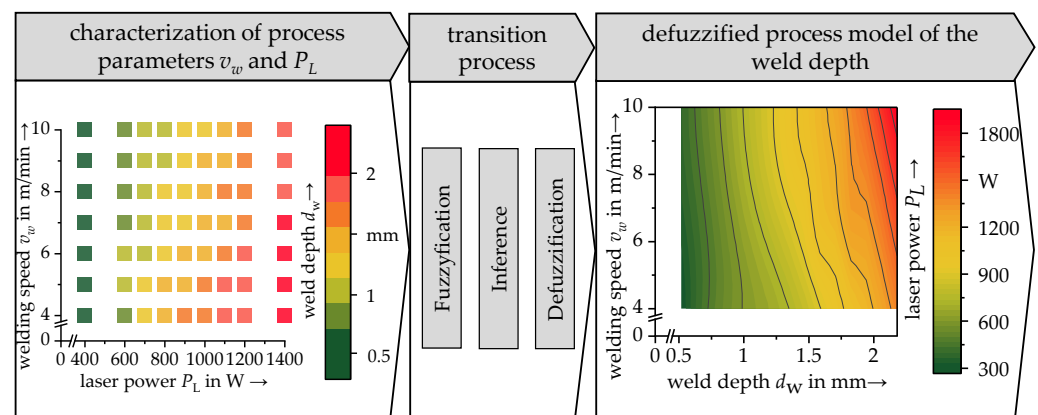


Figure 6. Transfer process of a discretized model for describing the relationships between the weld depth and process parameters into a defuzzified, continuous model as a basis for identifying appropriate controller reactions.

To meet the requirements of a highly flexible production system, the aim was to minimize changeover costs by reducing the effort for parameter adjustments. The neuro-fuzzy approach provided an effective method to model a non-linear system's behavior by a transparent description. Human-based expert knowledge was easily incorporated to tune the controller with little effort. To provide the fuzzy controller with a process model, fuzzy sets and the regarding membership functions needed to be generated from the data. Input and output parameter sets were additionally defined. To map the complex relationships between process parameters in laser beam welding, the membership functions for the fuzzy sets were derived by an Adaptive Neuro-Fuzzy Inference system (ANFIS) in Matlab.

With the help of the ANFIS, an optimal adjustment of the fuzzy membership functions was carried out. The available input and output data of the controlled process were the laser power, the feed rate and the weld depth, respectively. According to the control architecture and the choice of control variables, the input variables of the fuzzy controller were the target weld depth and the feed rate v_w , while the output was the laser power. First, the input and output behavior were linearly approximated. The intention was a minimization of the Root Mean Square Error (RMSE). The c-means clustering with backpropagation for the membership function of the input parameters and the least-squares algorithm for the membership functions of the output parameter showed the best adaption to the available data set. By a weighted average defuzzification, the process model was finally determined and integrated into the controller.

The overall structure of the control loop is shown in Figure 7. To operate the laser beam welding system, the user specified the desired weld depth. The pilot control, which contained the process model, determined the operating point of the laser power $P_{L,s}$ and feed rate v for the desired weld depth. Before the control system was activated, the parameter set was applied for 50 ms in an open-loop manner to stabilize deep penetration welding. After the closed-loop control was activated, the expected laser power P_L was calculated based on the reference model of the fuzzy-logic controller depending on the actual weld depth d_w . The corresponding deviation between the expected laser power and the setpoint laser power resulted in the laser power correction value ΔP_L . The correction value was limited around the setpoint. This saturation was used to prevent the control loop from being influenced by short-term process instabilities or errors in the signal. For this purpose, floating borders were determined experimentally, allowing for a maximum change in the laser power of 25 W between cycles.

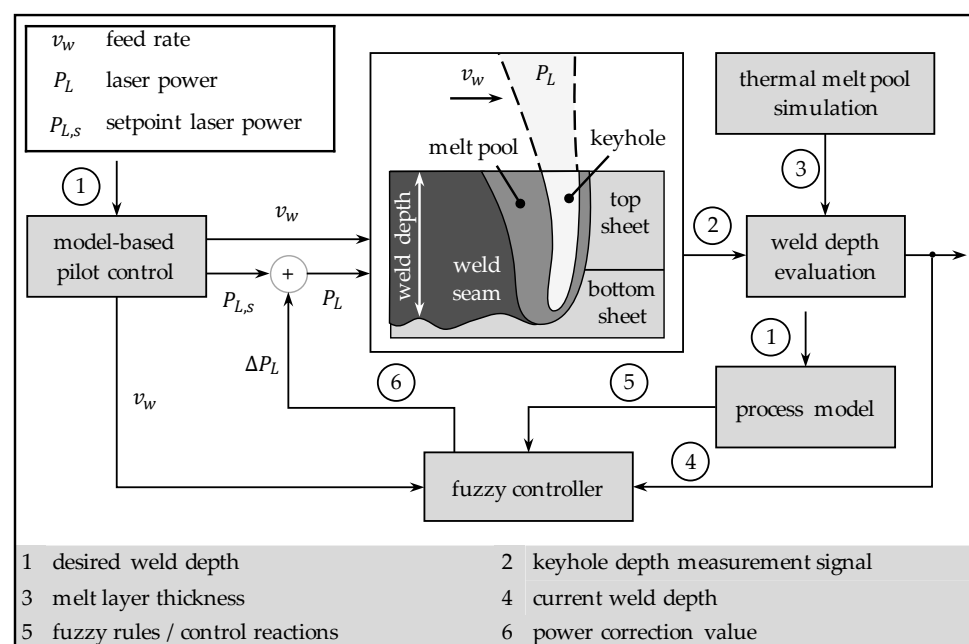


Figure 7. Structure of the weld depth control loop.

6. Experimental Validation and Discussion

For the validation of the predictions of the Feed Forward Neural Network (FFNN) and the weld depth control strategy, bead-on-plate welding tests on EN AW-6082 and AA2219 were carried out. Three desired weld depths, 1.5 mm, 1.8 mm and 2.0 mm, were selected for the investigation. For each weld depth, four welds were executed, whereby the controller settings were kept identical for the two materials. The angle of incidence of the welding optics was set to -10° (piercing process).

The implemented data processing algorithms provided new input data to the FFNN every 6 ms. The FFNN and the used laser beam source required 1 ms to estimate the weld depth and approximately 24 ms to adjust the laser power to the desired level, respectively. Thus, a shift between the position of the data acquisition along the weld seam direction and the adjusted weld depth belonging to the mentioned position could be identified. Due to the shift, a datapoint-related deviation calculation between the weld depth determined from the longitudinal cross-sections and the estimated weld depth of the FFNN was not practical. Instead, the mean value of the calculated deviation was used for the accuracy determination of the prediction and the control strategy overall. The mean value was calculated for every two welds with identical controller settings. For both materials, the welding experiments for the desired weld depth of 1.8 mm resulted in the most accurate approximation of the FFNN. The mean deviation between the approximated and the actual weld depth for EN AW-6082 was $109\ \mu\text{m}$, which corresponds to 6.1% of the desired weld depth. For the AA2219 material, the predictions of the FFNN were found to be more accurate, with a mean deviation of $31\ \mu\text{m}$, or 1.7% of the desired weld depth. Across all weld depths analyzed, the predictions of the FFNN, in general, were more accurate for the AA2219 than for the EN AW-6082 material. This higher accuracy is related to the fact that the FFNN was trained with data resulting from experiments using AA2219. Due to different alloy elements and consequently different material properties of EN AW-6082, higher deviations occurred. Nevertheless, the transferability and generalizability of the FFNN was proven, since it also provided sufficiently accurate predictions for the EN AW-6082 material. Further observations derived from the validations showed that with the proposed intelligent welding architecture, the welding process was more stable at 1.5 mm (cf. Figure 8) and 1.8 mm (cf. Figure 9) than at 2 mm (cf. Figure 10) of desired weld depth. It can be assumed that at the aforementioned lower weld depths, the keyhole remained more stable, resulting in a more accurate data acquisition by the OCT sensor with a higher signal-to-noise ratio. Based on the results, the conclusion can be drawn that the setting of the controller parameters for the level of increasing/decreasing the laser power are essential for a stabilization of the welding process and consequently achieving the desired weld depth. Unoptimized settings led to oscillations in the system due to the limited bandwidth of the control loop. These manifested themselves in the laser power signal, the OCT depth signal as well as the weld depth in the longitudinal cross-sections (cf. Figure 10). The oscillations were a consequence of the collapsing keyhole and, therefore, a poor data acquisition of the OCT sensor during an unstable welding process, where insufficiently precise characteristics could be derived from the signal as inputs for the FFNN. The following approximations of the FFNN were less accurate, and the output control values of the fuzzy controller did not correlate with the current process behavior. In addition, higher deviations between the desired and the actual weld depth due to non-optimal controller responses were the consequence.

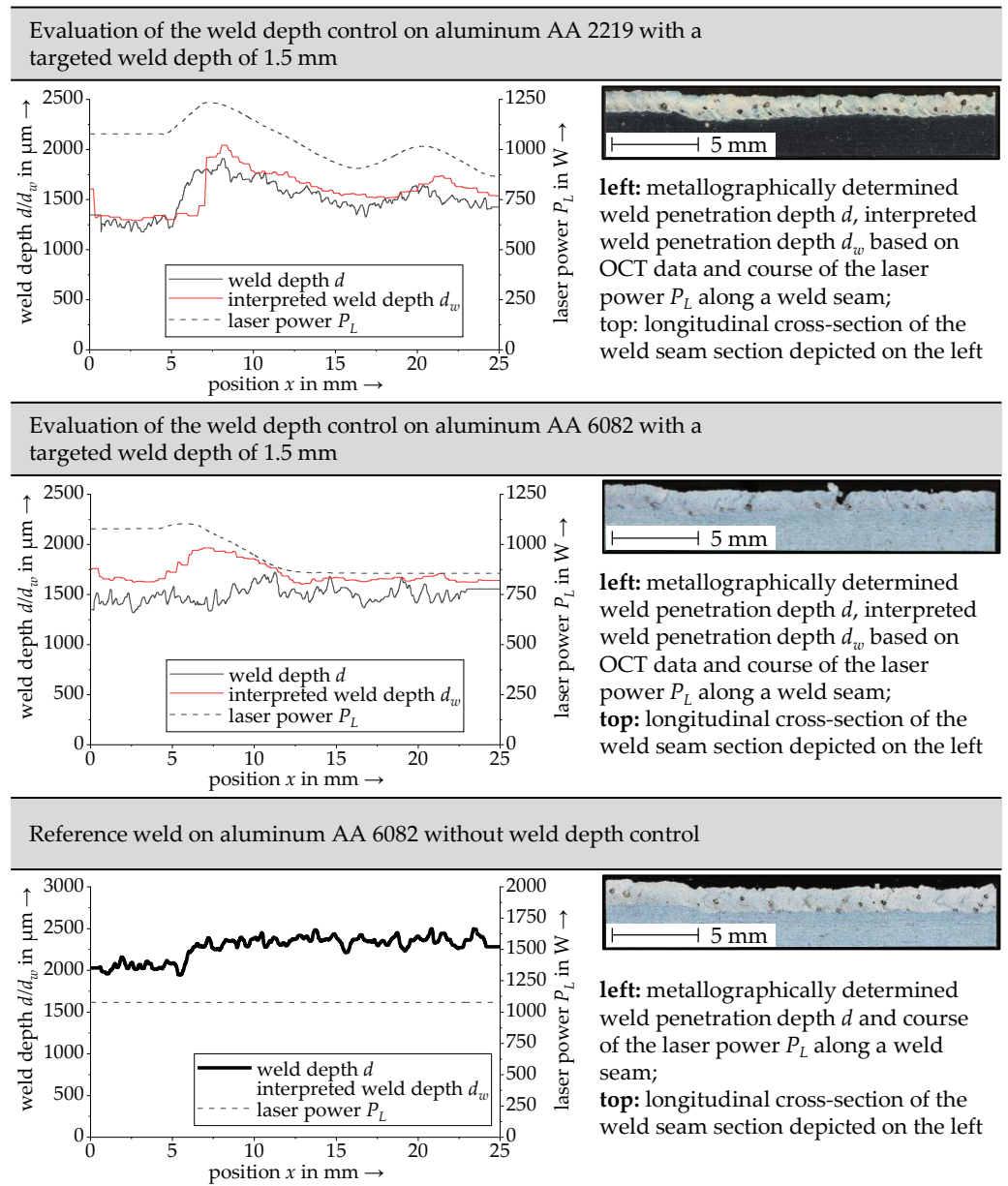


Figure 8. Comparison of the weld depth profiles for a targeted depth of 1.5 mm with a 300 μm deep notch for the aluminum alloy AA2219 with active weld depth control (top), for the aluminum alloy EN AW-6082 with active weld depth control and for the aluminum alloy EN AW-6082 without weld depth control.

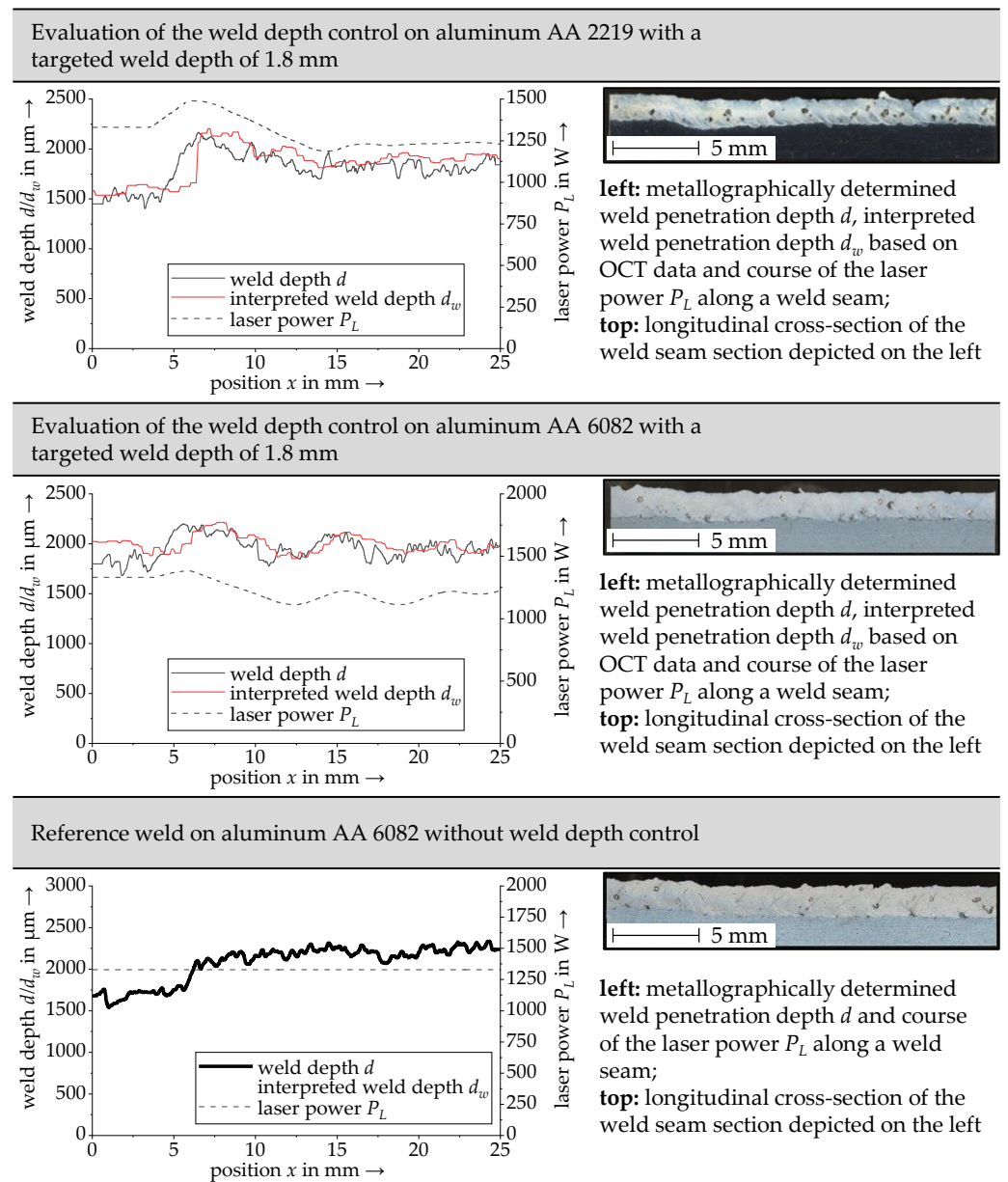


Figure 9. Comparison of the weld depth profiles for a targeted depth of 1.8 mm with a 300 μm deep notch for the aluminum alloy AA2219 with active weld depth control (top), for the aluminum alloy EN AW-6082 with active weld depth control and for the aluminum alloy EN AW-6082 without weld depth control.

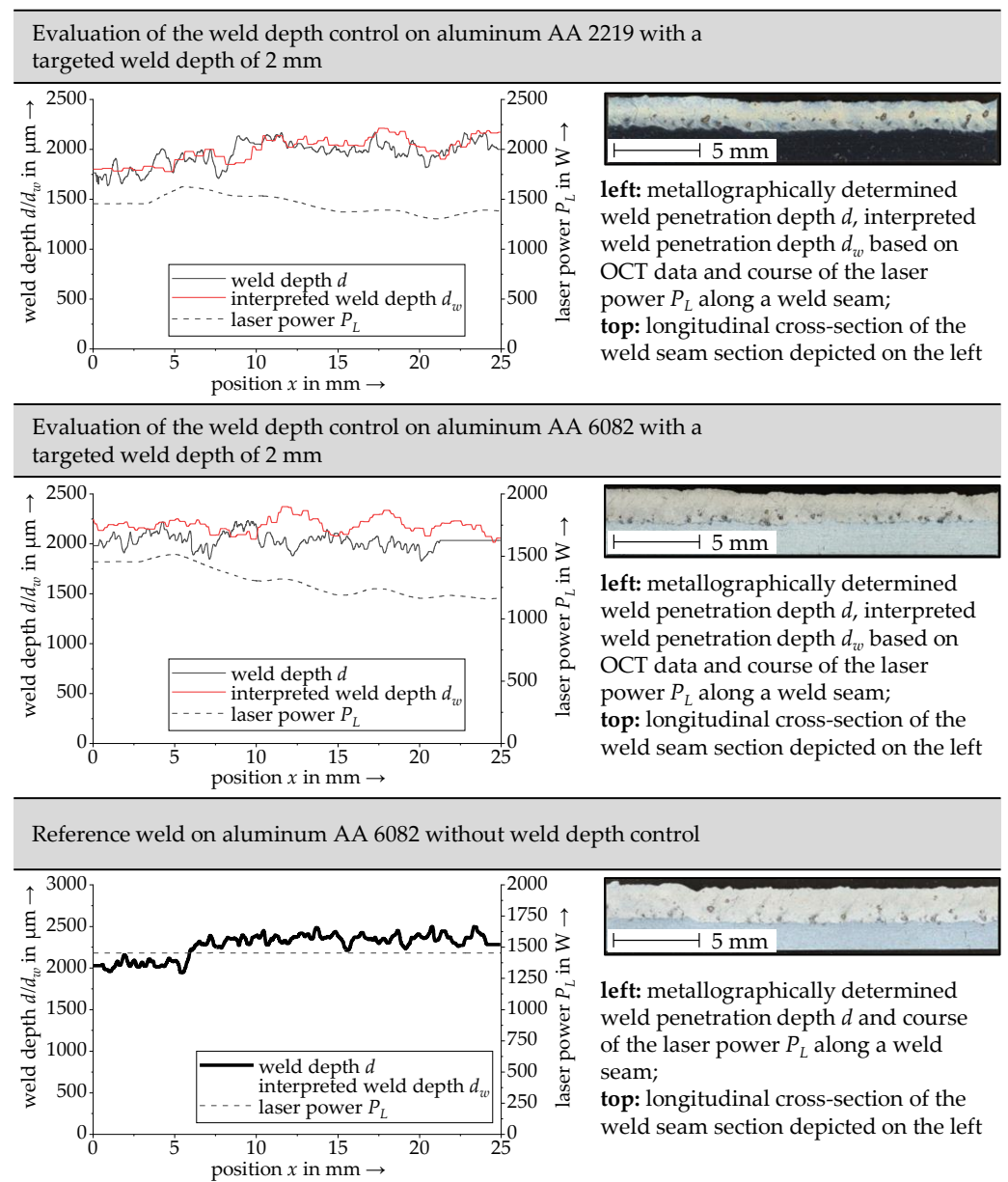


Figure 10. Comparison of the weld depth profiles for a targeted depth of 2.0 mm with a 300 μm deep notch for the aluminum alloy AA2219 with active weld depth control (top), for the aluminum alloy EN AW-6082 with active weld depth control and for the aluminum alloy EN AW-6082 without weld depth control.

7. Summary and Outlook

The experimental investigations in this work were performed using bead-on-plate welds. With this simplification, the influence of the joint geometry on the characteristics of the OCT signal was avoided, and keyhole depth measurements during laser beam welding could be systematically investigated. Based on the results, a weld depth control was presented which, depending on the penetration depth and the material of the weld specimens, allowed a reduction in the deviation between the specified targeted depth and the real depth to less than 6.1%. One way to extend the applicability of weld depth control to the reliable and flexible welding of two components in the future is to consider the joint geometry when determining the weld depth. This requires an extension of the algorithm for interpreting the OCT signal by including the joint geometry as an input variable. The results presented are, however, limited to the aluminum alloys EN AW-6082 and AA2219.

Measuring the keyhole depth in aluminum is considered more challenging compared to copper due to the high scattering of the OCT signal within the keyhole [8]. Future studies have the potential to enable the OCT-based evaluation and control of weld depth for a wider range of materials, such as steel or copper alloys. In addition, the weld penetration depth is an important process variable in the fabrication of components with joints of dissimilar metals. A common example with high relevance for e-mobility applications is the production of dissimilar joints between aluminum and copper components in an overlapping configuration. In this case, the weld depth control offers the potential to diminish the formation of intermetallic phases and thus the embrittlement of the weld seams by precisely controlling the capillary depth in order to avoid welding into the lower joining partner and thus intermixing.

For the presented weld depth control, the technological platform was a fixed optics system with an integrated OCT sensor unit. The use of fixed optics is widespread in industrial applications such as car body or battery storage manufacturing. However, for brilliant laser radiation with small focal diameters and high intensities, galvanometer scanning optics are preferred in industrial applications. For the use of the weld depth control in combination with a scanning optics system, several technical enhancements are necessary. In particular, a highly dynamic positioning of the OCT measuring spot relative to the focal point of the processing laser is required since the relative positioning accuracy of the measuring and processing spot depends on the accuracy of the scanning system. Consequently, a calibration method for the measurement system must be provided to position the OCT focal point over the entire processing field of the scanning optics.

Author Contributions: Conceptualization, M.S., C.S.; Data curation, M.S., K.G.; Formal analysis, M.S., C.B.; Funding acquisition, C.S., M.F.Z.; Investigation, M.S., T.W., K.G.; Methodology, M.S., C.B.; Project administration, M.S., C.S., M.F.Z.; Resources, M.F.Z.; Software, T.W.; Supervision, M.F.Z.; Validation, M.S., T.W., C.B.; Visualization, M.S.; Writing—original draft, M.S., T.W., C.S.; Writing—review & editing, M.S., T.W., K.G., C.S., C.B., M.F.Z. All authors have read and agreed to the published version of the manuscript.

Funding: This research was funded by the German Federal Ministry of Education and Research (BMBF) within the Photonics Research Germany funding program under the grant number 13N14555. The APC was funded by the Federal Ministry for Economic Affairs and Climate Action under the grant number 13IK002L.

Institutional Review Board Statement: Not applicable.

Informed Consent Statement: Not applicable.

Data Availability Statement: Not applicable.

Acknowledgments: The results presented were achieved within the RoKtoLas project, which was supported by the German Federal Ministry of Education and Research (BMBF) within the Photonics Research Germany funding program (contract number 13N14555) and supervised by the VDI Technology Center (VDI TZ). We would like to thank the BMBF and the VDI TZ for their support and for the effective and trusting cooperation.

Conflicts of Interest: The authors declare no conflict of interest.

References

1. Stadter, C.; Schmoeller, M.; Zeitler, M.; Tueretkan, V.; Munzert, U.; Zaeh, M.F. Process control and quality assurance in remote laser beam welding by optical coherence tomography. *J. Laser Appl.* **2019**, *31*, 22408. [[CrossRef](#)]
2. Mayr, A.; Lutz, B.; Weigelt, M.; Glabel, T.; Kibkalt, D.; Masuch, M.; Riedel, A.; Franke, J. Evaluation of Machine Learning for Quality Monitoring of Laser Welding Using the Example of the Contacting of Hairpin Windings. In Proceedings of the 8th International Electric Drives Production Conference (EDPC), Schweinfurt, Germany, 4–5 December 2018; pp. 1–7, ISBN 9781728101484.
3. Schaumberger, K.; Beck, M.; Saffer, J.; Kaufmann, F.; Ermer, J.; Roth, S.; Schmidt, M. Improving process reliability by means of detection of weld seam irregularities in copper via thermographic process monitoring. *Procedia Manuf.* **2019**, *36*, 58–63. [[CrossRef](#)]
4. Boley, M.; Fetzer, F.; Graf, T.; Weber, R. High-speed x-ray imaging system for the investigation of laser welding processes. *J. Laser Appl.* **2019**, *31*, 042004-1–042004-10. [[CrossRef](#)]

5. Purtonen, T.; Kalliosaari, A.; Salminen, A. Monitoring and Adaptive Control of Laser Processes. *Phys. Procedia* **2014**, *56*, 1218–1231. [[CrossRef](#)]
6. Bautze, T.; Kogel-Hollacher, M. Keyhole Depth is just a Distance. *Laser Tech. J.* **2014**, *11*, 39–43. [[CrossRef](#)]
7. Stadter, C.; Schmoeller, M.; von Rhein, L.; Zaeh, M.F. Real-time prediction of quality characteristics in laser beam welding using optical coherence tomography and machine learning. *J. Laser Appl.* **2020**, *32*, 22046. [[CrossRef](#)]
8. Schmoeller, M.; Stadter, C.; Liebl, S.; Zaeh, M.F. Inline weld depth measurement for high brilliance laser beam sources using optical coherence tomography. *J. Laser Appl.* **2019**, *31*, 22409. [[CrossRef](#)]
9. Kogel-Hollacher, M.; Schoenleber, M.; Schulze, J.; Bautze, T.; Strebel, M.; Moser, R. Inline measurement for quality control from macro to micro laser applications (Conference Presentation). In *High-Power Laser Materials Processing: Applications, Diagnostics, and Systems VI*; SPIE: Bellingham, WA, USA, 2017; Volume 10097, pp. 100910H-1–100910H-9. [[CrossRef](#)]
10. Sokolov, M.; Franciosa, P.; Al Botros, R.; Ceglarek, D. Keyhole mapping to enable closed-loop weld penetration depth control for remote laser welding of aluminum components using optical coherence tomography. *J. Laser Appl.* **2020**, *32*, 32004. [[CrossRef](#)]
11. Webster, P.J.L.; Wright, L.G.; Ji, Y.; Galbraith, C.M.; Kinross, A.W.; van Vlack, C.; Fraser, J.M. Automatic laser welding and milling with in situ inline coherent imaging. *Opt. Lett.* **2014**, *39*, 6217–6220. [[CrossRef](#)]
12. Stadter, C.; Kick, M.K.; Schmoeller, M.; Zaeh, M.F. Correlation analysis between the beam propagation and the vapor capillary geometry by machine learning. *Procedia CIRP* **2020**, *94*, 742–747. [[CrossRef](#)]
13. Aktepe, A.; Ersöz, S.; Lüy, M. Welding Process Optimization with Artificial Neural Network Applications. *Neural Netw. World* **2014**, *24*, 655–670. [[CrossRef](#)]
14. Günther, J.; Pilarski, P.M.; Helfrich, G.; Shen, H.; Diepold, K. Intelligent laser welding through representation, prediction, and control learning: An architecture with deep neural networks and reinforcement learning. *Mechatronics* **2015**, *34*, 1–11. [[CrossRef](#)]
15. Zhang, Z.; Li, B.; Zhang, W.; Lu, R.; Wada, S.; Zhang, Y. Real-time penetration state monitoring using convolutional neural network for laser welding of tailor rolled blanks. *J. Manuf. Syst.* **2020**, *54*, 348–360. [[CrossRef](#)]
16. Zhang, Y.; You, D.; Gao, X.; Wang, C.; Li, Y.; Gao, P.P. Real-time monitoring of high-power disk laser welding statuses based on deep learning framework. *J. Intell. Manuf.* **2020**, *31*, 799–814. [[CrossRef](#)]
17. Blug, A.; Abt, F.; Nicolosi, L.; Heider, A.; Weber, R.; Carl, D.; Höfler, H.; Tetzlaff, R. The full penetration hole as a stochastic process: Controlling penetration depth in keyhole laser-welding processes. *Appl. Phys. A* **2012**, *108*, 97–107. [[CrossRef](#)]
18. Blug, A.; Carl, D.; Höfler, H.; Abt, F.; Heider, A.; Weber, R.; Nicolosi, L.; Tetzlaff, R. Closed-loop Control of Laser Power using the Full Penetration Hole Image Feature in Aluminum Welding Processes. *Phys. Procedia* **2011**, *12*, 720–729. [[CrossRef](#)]
19. Bardin, F.; Cobo, A.; Lopez-Higuera, J.M.; Collin, O.; Aubry, P.; Dubois, T.; Högrström, M.; Nylen, P.; Jonsson, P.; Jones, J.D.C.; et al. Closed-loop power and focus control of laser welding for full-penetration monitoring. *Appl. Opt.* **2005**, *44*, 13–21. [[CrossRef](#)]
20. Birnesser, A.J. *Prozessregelung beim Laserstrahlschweißen*; Universität Stuttgart: München, Germany, 2011; ISBN 9783831641338.
21. Konuk, A.; Aarts, R.; Veld, A.H.I.; Sibillano, T.; Rizzi, D.; Ancona, A. Process Control of Stainless Steel Laser Welding using an Optical Spectroscopic Sensor. *Phys. Procedia* **2011**, *12*, 744–751. [[CrossRef](#)]
22. Kos, M.; Arko, E.; Kosler, H.; Jezeršek, M. Penetration-depth control in a remote laser-welding system based on an optical triangulation loop. *Opt. Lasers Eng.* **2021**, *139*, 106464-1–106464-14. [[CrossRef](#)]
23. Michel, J. *Approximatives Modell für das Tiefschweißen mit Laserstrahlung*; RWTH Aachen: Aachen, Germany, 2004; ISBN 3832224076.
24. Bollig, A.; Mann, S.; Beck, R.; Kaieler, S. Einsatz optischer Technologien zur Regelung des Laserstrahlschweißprozesses. *Automatisierungstechnik* **2005**, *53*, 513–521. [[CrossRef](#)]
25. Liu, Y.; Zhang, W.; Zhang, Y. Dynamic Neuro-Fuzzy-Based Human Intelligence Modeling and Control in GTAW. *IEEE Trans. Autom. Sci. Eng.* **2015**, *12*, 324–335. [[CrossRef](#)]
26. Schmoeller, M.; Stadter, C.; Kick, M.; Geiger, C.; Zaeh, M.F. A Novel Approach to the Holistic 3D Characterization of Weld Seams—Paving the Way for Deep Learning-Based Process Monitoring. *Materials* **2021**, *14*, 6928. [[CrossRef](#)]
27. Mertins, A. *Signaltheorie: Grundlagen der Signalbeschreibung, Filterbänke, Wavelets, Zeit-Frequenz-Analyse, Parameter- und Signalschätzung*, 4th ed.; Springer Fachmedien Wiesbaden: Wiesbaden, Germany, 2020; ISBN 9783658296483.
28. Kim, H.; Melhem, H. Fourier and wavelet analyses for fatigue assessment of concrete beams. *Exp. Mech.* **2003**, *43*, 131–140. [[CrossRef](#)]
29. Cariolaro, G. *Unified Signal Theory*; Springer: Heidelberg, Germany, 2011; ISBN 9780857294630.
30. Schmoeller, M.; Neureiter, M.; Stadter, C.; Zaeh, M.F. Numerical weld pool simulation for the accuracy improvement of inline weld depth measurement based on optical coherence tomography. *J. Laser Appl.* **2020**, *32*, 22036. [[CrossRef](#)]
31. Schmoeller, M.; Stadter, C.; Wagner, M.; Zaeh, M.F. Investigation of the influences of the process parameters on the weld depth in laser beam welding of AA6082 using machine learning methods. *Procedia CIRP* **2020**, *94*, 702–707. [[CrossRef](#)]
32. Hagenlocher, C.; Fetzter, F.; Weber, R.; Graf, T. Benefits of very high feed rates for laser beam welding of AlMgSi aluminum alloys. *J. Laser Appl.* **2018**, *30*, 12015. [[CrossRef](#)]